Maximum Terminal Velocity Turns at Nearly Constant Altitude

G. Richard Eisler*
Sandia National Laboratories, Albuquerque, New Mexico
and
David G. Hull†
University of Texas, Austin, Texas

An optimal control problem is formulated for a maneuvering re-entry vehicle to execute a maximum terminal velocity turn at constant altitude to a fixed final position. A control solution technique is devised that uses a Newton scheme to repetitively solve a nonlinear algebraic system for two parameters to provide the on-line guidance. The turn control takes advantage of the high dynamic pressure at the beginning of the flight path; the lift solution acts to null deviations from the prescribed altitude. Control solutions are compared for an approximate physical model, for a simulation of the approximate optimal guidance in a true physical model, and for a parameter optimization solution for the true model. End constraint satisfaction is excellent and overall trajectory agreement is good, if the assumed atmospheric model is reasonably accurate.

Nomenclature

C_D, C_L, C_S = drag, lift, and side force coefficients
C_{D_0} = zero-lift drag coefficient
C_L^* = lift coefficient at maximum L/D
f = nonlinear algebraic equation
F, E = elliptic integrals of the first and second kinds
g = gravitational acceleration, ft/s^2
G, H = end function and Hamiltonian
h = altitude above mean sea level, ft
I = elliptic integral in Eq. (26)
J = performance index
k = elliptic integral modulus
m = mass, slugs, $\sqrt{q^2+r^2}$ in elliptic integral formulas
$M, \bar{M}$ = sum of centrifugal and gravitational terms in the flight path angle equation
$p_u, p_w, p_x, p_y, p_z, p_\gamma$ = Lagrange multipliers for state equations
p, q, r = turn control constants in Eq. (19)
r = distance from center of Earth, ft
R = nondimensional standoff range to target
S_R = vehicle reference area, ft
t = time, s
u = negative logarithm of velocity
V = velocity, ft/s
w = nondimensional density
X', Y', Z' = Earth-centered inertial coordinate directions
x', y', z' = local horizon coordinate directions
X, Y = inertial downrange and crossrange, n.mi.
x, y, z = nondimensional downrange, crossrange, and altitude
β = atmospheric scale height, ft
γ, χ = flight path and heading angles, rad
θ, ϕ = inertial longitude and latitude angles, rad
κ = fit constant in quadratic drag polar
λ, σ = scaled lift and side force coefficients
ν = Lagrange multipliers for end constraints
ρ = atmospheric density, slugs/ft^3
Φ = elliptic integral argument

Subscripts

f = final
s = mean sea level
T = target
0 = initial

Received Feb. 9, 1987; revision received June 3, 1987. This paper is declared a work of the U.S. Government and therefore is in the public domain.

*Member of the Technical Staff, Aerodynamics Department. Senior Member AIAA.
†M.J. Thompson Regents Professor, Department of Aerospace Engineering. Associate Fellow AIAA.

Introduction

TO enable the widest field of view for body-fixed radars or to maintain flight condition consistency for onboard experiments, it is desirable for a maneuvering re-entry vehicle to fly in the vicinity of a constant altitude. Active radars may need to survey large expanses to acquire possible targets. High-altitude research experiments for aerospaceplane-type concepts may wish to acquire data over a range of Mach numbers at a consistent altitude.

Maximizing the terminal velocity of a turn to a point has the dual advantage of reducing the time to reach the position as well as maximizing the kinetic energy level for any subsequent maneuvers. This paper describes guidance schemes for atmospheric flight of a hypersonic re-entry vehicle that executes a near-constant-altitude, maximum terminal velocity (MTV) turn. The maneuver is terminated by either aligning the velocity vector with a target point at a desired standoff range or, as a limiting case, flying to the target point.

The purpose of this study is to find approximate, optimal control rules that can be computed repetitively to provide real-time, MTV guidance. The solution is derived from an integrable system of equations in terms of the heading angle. Since flying precisely at constant altitude is usually not possible simply due to atmospheric disturbances, lift corrections for deviations are a necessary part of the solution.

The control computations are implemented in a sample data guidance scheme and results are compared between a continuously updated physical model and a true or *simulation* physical model. These two results are compared with a parameter optimization control solution for the simulation physical model.

Approximations to the Equations of Motion

The simulation physical model is the system of differential equations describing the motion of a nonthrusting, point mass

with respect to a nonrotating, spherical Earth.[1] The velocity vector of the *skid-to-turn* vehicle is described in a local horizon frame moving with respect to an Earth-centered inertial frame (Fig. 1). As in Ref. 1, the following approximations are made:

1) $h \ll r_s$.
2) ϕ small.
3) $V\cos\gamma\cos\chi\tan\phi/(r_s+h)$ negligible.
4) $g_s|\sin\gamma| \ll D/m$.
5) $C_D = C_{D_0} + \kappa C_S^2 + \kappa C_L^2$.

Two further approximations for flight near a constant altitude are that

6) γ is small (i.e., $\cos\gamma \approx 1$, $\sin\gamma \approx \gamma$).
7) ρ is constant. (Since this problem will be solved repetitively, the value of ρ will be assigned from an *exponential* model,[2] $\rho = \rho_s e^{-h/\beta}$, where $\rho_s = 0.002376$ slugs/ft^3, $\beta = 23{,}800$ ft, and h is the current altitude.)

The last approximation is associated with the centrifugal and gravitational term

$$M = \left[1 - \frac{g_s r_s^2}{V^2(r_s+h)}\right]\frac{1}{\rho(r_s+h)}$$

which appears on the right-hand side of the $\dot{\gamma}$ equation. This term is clearly a function of V and can double or triple in magnitude over the extent of the trajectory. The presence of this term makes it impossible to solve the optimal control problem analytically and some approximation is needed. One approach is to neglect the term by assuming that aerodynamic forces dominate. However, it is important for gravity to appear in some form, so the approach used here is to assume some value for the term and hold it constant over the trajectory. An average value would be desirable; however, only the initial value is available, so it is used instead. In applying the results from this study as a guidance law, the value of this term is continuously updated, giving it the character of an average value. With these approximations, the following physical model is produced:

$$\dot{X} = V\cos\chi \tag{1}$$

$$\dot{Y} = V\sin\chi \tag{2}$$

$$\dot{h} = V\gamma \tag{3}$$

$$\dot{V} = -\rho V^2 S_R C_{D_0}(1+\sigma^2+\lambda^2)/2m \tag{4}$$

$$\dot{\gamma} = \rho V C_L^* S_R(\lambda+\bar{M})/2m \tag{5}$$

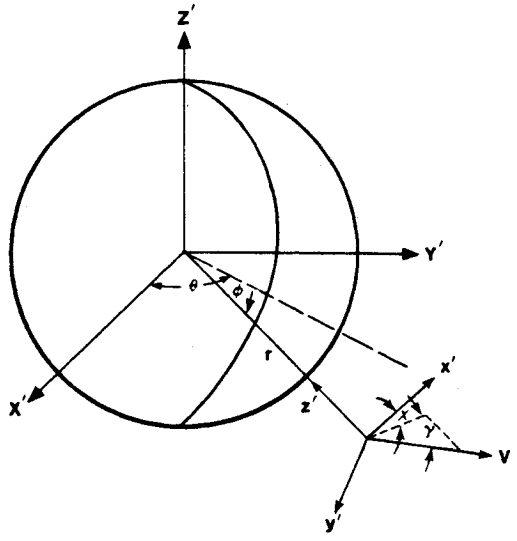

Fig. 1 Coordinate systems.

$$\dot{\chi} = \rho V C_L^* S_R \sigma/2m \tag{6}$$

where

$$(\dot{}) = \frac{\mathrm{d}(\ )}{\mathrm{d}t}, \quad X = r_s\theta, \quad Y = r_s\phi, \quad \sigma = \frac{C_S}{C_L^*}$$

$$\lambda = \frac{C_L}{C_L^*}, \quad C_L^* = \left(\frac{C_{D_0}}{\kappa}\right)^{1/2}, \quad \bar{M} = \frac{2mM}{C_L^* S_R}$$

Note that the complete set of position variables (X,Y,h) has been retained, since the final position is constrained.

Since there is no boundary condition on the independent variable, time, it can be eliminated in favor of χ, which also varies monotonically. Suitable nondimensional states chosen to replace X, Y, h, ρ, and V are

$$x,y,z = \frac{(X,Y,h)}{\beta}, \quad w = \frac{\rho}{2m/(\beta S_R C_L^*)}, \quad u = -\left(\frac{C_L^*}{C_{D_0}}\right)\ln V \tag{7}$$

Maximizing velocity now entails *minimizing* u. With these changes, the state equations used in the optimal control problem are

$$\frac{\mathrm{d}x}{\mathrm{d}\chi} = \frac{\cos\chi}{w\sigma} \tag{8}$$

$$\frac{\mathrm{d}y}{\mathrm{d}\chi} = \frac{\sin\chi}{w\sigma} \tag{9}$$

$$\frac{\mathrm{d}z}{\mathrm{d}\chi} = \frac{\gamma}{w\sigma} \tag{10}$$

$$\frac{\mathrm{d}u}{\mathrm{d}\chi} = \frac{1+\sigma^2+\lambda^2}{\sigma} \tag{11}$$

$$\frac{\mathrm{d}\gamma}{\mathrm{d}\chi} = \frac{\lambda+\bar{M}}{\sigma} \tag{12}$$

Optimal Control Problem

The goal is to maximize terminal velocity while maintaining flight about a desired altitude to a constrained terminal position. It is assumed that the vehicle is initially flying at the desired altitude with a near-level velocity orientation. The problem is formulated as a turn to a circle of radius R, as shown in Fig. 2. The end point of the trajectory (x_f,y_f,z_f) is such that the velocity vector is aligned with the target point (x_T,y_T,z_T) at a specified standoff range R at the target altitude $(z_f = z_T)$.

$$\lim_{R\to 0} x_f = x_T \quad \text{and} \quad \lim_{R\to 0} y_f = y_T$$

This limiting case is a *turn to a point*. Nearness to the target altitude is also maintained by constraining γ_f to zero.

In formal terms, the problem consists of minimizing the performance index,

$$J = u_f$$

subject to

State equations: Eqs. (8-12)

Initial conditions: $\chi_0 x_0 y_0 z_0 u_0 \gamma_0$ known

Final conditions: $(x_T - x_f)^2 + (y_T - y_f)^2 = R^2$

$$\tan\chi_f = (y_T - y_f)/(x_T - x_f)$$

$$Z_f = Z_T, \qquad \gamma_f = 0$$

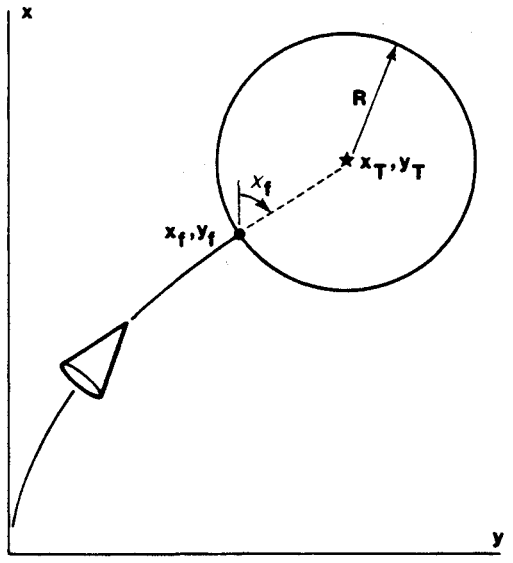

Fig. 2 Engagement geometry.

From these, the Hamiltonian and end function can be constructed as

$$H=\frac{1}{\sigma}\left[\frac{p_x\cos\chi+p_y\sin\chi+p_z\gamma}{w}+p_u(1+\sigma^2+\lambda^2)+p_\gamma(\lambda+\bar{M})\right] \tag{13}$$

$$G=u_f+\nu_1[(x_T-x_f)^2+(y_T-y_f)^2-R^2]+\nu_2[\tan\chi_f(x_T-x_f)-(y_T-y_f)]+\nu_3(z_f-z_T)+\nu_4(\gamma_f) \tag{14}$$

Since χ is the independent variable, γ is the only state to appear in H and, as such, all Lagrange multipliers except p_γ are constants. p_γ varies as

$$\frac{dp_\gamma}{d\chi}=-H_\gamma=-\frac{p_z}{w\sigma}\quad(p_{\gamma_f}=\nu_4) \tag{15}$$

and the multiplier constants are obtained from the following natural boundary relations:

$$p_x=-2\nu_1(x_T-x_f)-\nu_2\tan\chi_f,\quad p_y=-2\nu_1(y_T-y_f)+\nu_2$$
$$p_z=\nu_3,\quad p_u=1 \tag{16}$$

The control equations, $H_\sigma=H_\lambda=0$, give the following:

$$\sigma^2=1+p_\gamma\bar{M}-p_\gamma^2/4+p_z\gamma/w+(p_x\cos\chi+p_y\sin\chi)/w \tag{17}$$

$$\lambda=-p_\gamma/2 \tag{18}$$

where the sign of σ is dictated by the turn direction. If the expression for σ^2 is differentiated, it is seen that the first four terms form a constant p and the control law can be restated as

$$\sigma^2=p+q\cos\chi-r\sin\chi \tag{19}$$

where

$$p=1+p_\gamma\bar{M}-p_\gamma^2/4+p_z\gamma/w \tag{20}$$

$q=p_x/w$, and $r=-p_y/w$.

The boundary condition for χ_f free, $G_{x_f}+H_f=0$, produces

$$\nu_2(x_T-x_f)\sec^2\chi_f+2\sigma_f=0 \tag{21}$$

In addition to these conditions, a first integral can be derived by differentiating Eq. (19), rearranging the result, and integrating from χ_0 to χ_f to give

$$2(\sigma_f-\sigma_0)=-w[q(y_f-y_0)+r(x_f-x_0)] \tag{22}$$

This is similar to one previously found by Vinh.[3]

Solution of the State Equations

Using the control forms in Eqs. (18) and (19) allows the integration of the complete set of state equations (8–12). The solutions for the ranges x and y result from integrating the following:

$$\frac{dx}{d\chi}=\frac{\cos\chi}{\pm w[p+q\cos\chi-r\sin\chi]^{1/2}}$$
$$\frac{dy}{d\chi}=\frac{\sin\chi}{\pm w[p+q\cos\chi-r\sin\chi]^{1/2}} \tag{23}$$

to produce

$$x_f-x_0=\frac{1}{\pm w}\left[\frac{\sqrt{2}q}{m^{3/2}}[2E(\Phi,k)-F(\Phi,k)]-\frac{2r}{m^2}\sigma\right]_{x_0}^{x_f}$$
$$y_f-y_0=\frac{1}{\pm w}\left[\frac{\sqrt{2}(-r)}{m^{3/2}}[2E(\Phi,k)-F(\Phi,k)]-\frac{2q}{m^2}\sigma\right]_{x_0}^{x_f} \tag{24}$$

The $\pm$ sign indicates the turn direction, + for positive heading change. F, E are elliptic integrals[4] of the first and second kinds and

$$\Phi=\sin^{-1}\left[\frac{p-q\cos\chi+r\sin\chi}{p+m}\right]^{1/2},\quad -k=\left[\frac{p+m}{2m}\right]^{1/2}$$
$$m=\sqrt{q^2+r^2}$$

The vertical plane variables γ and z can be found once p_γ is known. If Eq. (19) is substituted into Eq. (15), the result is

$$\frac{dp_\gamma}{d\chi}=\frac{-p_z}{\pm w[p+q\cos\chi-r\sin\chi]^{1/2}} \tag{25}$$

which can be integrated to give

$$p_{\gamma_f}-p_{\gamma_0}=-\frac{p_z}{\pm w}I(\chi_f) \tag{26}$$

where

$$I(\chi_f)=\sqrt{\frac{2}{m}}F(\Phi,k)\Big|_{x_0}^{x_f} \tag{27}$$

The following integrals can then be formed between γ, z, and p_γ:

$$\gamma_f-\gamma_0=\frac{w(p_{\gamma_f}-p_{\gamma_0})}{p_z}\left[\frac{p_{\gamma_f}+p_{\gamma_0}}{4}-\bar{M}\right] \tag{28}$$

$$z_f-z_0=\frac{w(p_{\gamma_f}-p_{\gamma_0})^2}{p_z^2}\left[\frac{\bar{M}}{2}-\frac{p_{\gamma_f}+2p_{\gamma_0}}{12}\right]-\frac{\gamma_0}{p_z}(p_{\gamma_f}-p_{\gamma_0}) \tag{29}$$

For z_f, γ_f fixed, Eqs. (26), (28), and (29) are combined to find p_z, p_{γ_0}, and p_{γ_f}. If the vehicle is flying in a true constant-

density medium, then it is appropriate to solve for the multipliers for any desired combination of z_f and γ_f (i.e., fixed or free).

Evaluation of the Lagrange Multipliers

To generate the steering commands in Eqs. (18) and (19), it is necessary to solve for the Lagrange multipliers, p_x, p_y, p_z, and p_{γ_0}. However, in order to isolate these, the general system of state equations and boundary conditions must be algebraically reduced. To begin, replace the unknown final ranges x_f and y_f in Eqs. (22) and (24) with $x_T - R\cos\chi_f$ and $y_T - R\sin\chi_f$. Combine Eqs. (16), (21), and (22) to give

$$2\sigma_0 = p_x\Delta y - p_y\Delta x = w(q\Delta y + r\Delta x) \tag{30}$$

$$\sigma_f = R(p_x\sin\chi_f - p_y\cos\chi_f)/2 = Rw(q\sin\chi_f + r\cos\chi_f)/2 \tag{31}$$

where $\Delta x = x_T - x_0$ and $\Delta y = y_T - y_0$ are known. Note the

$$\lim_{R\to 0}\sigma_f = 0$$

σ_0 and σ_f are then eliminated by evaluating Eq. (19) at the appropriate χ and substituting for each one.

Equations (26), (28), and (29) can be combined to yield

$$p_z = (12w/I^2)(\gamma_0 - 2w\Delta z/I) \tag{32}$$

$$p_{\gamma_0} = 8\gamma_0/I + 2\bar{M} - 12w\Delta z/I^2 \tag{33}$$

where $\gamma_f = 0$ and $\Delta z = z_T - z_0$. If the constant p is evaluated at χ_0, then Eqs. (20), (24), and (30-34) form a nonlinear system of equations in six unknowns, p, q, r, χ_f, p_z, and p_{γ_0}.

A Newton's method is used to solve this nonlinear system. If values are assumed for two of the unknowns, q and r, then algebraic solutions can be obtained for the rest. To begin, initial values of q, r are generated from a completely algebraic solution for a similar problem in which χ is assumed small.[5] Equations (30) and (31) are squared and solved for p and χ_f. $I(\chi_f)$ is then computed and used in Eqs. (32) and (33) to obtain values for p_z and p_{γ_0}. These test values for the unknowns are verified in the following:

$$f_1(q,r) = p - (1 + p_{\gamma_0}\bar{M} - p_{\gamma_0}^2/4 + p_z\gamma_0/w)$$

$$f_2(q,r) = \Delta y - \left(R\sin\chi_f - \frac{1}{\pm w}\left\{\frac{\sqrt{2}(-r)}{m^{3/2}}[2E(\Phi,k) - F(\Phi,k)] - \frac{2q}{m^2}\sigma\right\}_{\chi_0}^{\chi_f}\right) \tag{34}$$

If f_1 and f_2 are not sufficiently close to zero, the constants q and r are incremented until convergence is achieved.

Once q and r have been found, an approximate optimal trajectory and control histories can be computed for a single value of $\bar{M}$ from the current initial conditions to the specified final conditions. In an actual sample data guidance setting, the problem is solved at each sample point along the trajectory, updating initial conditions and the approximate physical model via $\bar{M}$ with information received from onboard inertial measurement units.

Results

The objective of this study has been to develop a guidance law for the near-constant-altitude flight of a maneuverable hypersonic vehicle. To illustrate the effectiveness of the guidance law, three trajectories are calculated:

1) The guided trajectory based on the approximate equations of motion (1-6), the exponential atmosphere, and the quadratic drag polar. At each sample time, the state of the vehicle (h, V) is used to compute $\bar{M}$, the optimal controls are computed, and the controls are held fixed over the sample period ($\Delta t = 0.1$ s) at the value of the sample time. Hence, $\bar{M}$ is updated along the trajectory. This trajectory is calculated to see how the guidance law performs with the physical model from which it was developed.

2) The guided trajectory based on the simulation physical model. The simulation model includes the exact equations of motion, the standard atmosphere and aerodynamics for the skid-to-turn vehicle used in Ref. 1. Again, the optimal controls are held fixed over the sample period. This trajectory is meant to be representative of what might be obtained for a real vehicle.

3) The optimal constant-altitude trajectory. This trajectory is based on the simulation model and represents the best that could have been done in the true, constant-altitude flight of an actual vehicle.

In computation 1, the heading angle is used as the independent variable. However, for updating and comparison purposes, it is convenient to create a time/heading angle base for these computations using the Euler form

$$\chi(t_{k+1}) = \chi(t_k + \Delta t) = \chi(t_k) + \dot{\chi}(t_k)\Delta t \tag{35}$$

where $\dot{\chi}$ is given in Eq. (6). This is necessary in computation 1 where $\bar{M}$ is updated every Δt to reflect the changes in V, γ, and ρ. Computation 2 provides its own time base using a fourth-order Runge-Kutta integrator on the simulation equations of motion. The method of recursive quadratic programming developed by Powell[6] and contained in the parameter-optimization code, VFO2AD, is used to generate the trajectory results in computation 3. The parameters are the side force coefficients C_S at 11 points (*node* points) along the trajectory.[7] Linear interpolation is used to compute controls between nodes. Each parameter is perturbed and trajectory-based numerical derivatives of the performance index and constraints are computed. Lift coefficient C_L for the VFO2AD applications is obtained by solving $\dot{\gamma} = 0$ in Eq. (5) for $\bar{M}$ continuously variable.

The trajectory initial conditions are

$$X_0 = 0 \text{ n.mi.} \quad h_0 = 100{,}000 \text{ ft} \quad \gamma_0 = 0.1 \text{ deg}$$

$$Y_0 = 0 \text{ n.mi.} \quad V_0 = 11{,}300 \text{ ft/s} \quad \chi_0 = 0 \text{ deg}$$

For the VFO2AD results, $\gamma_0 = 0$ deg is used to compute the optimum velocity for true level flight. Results are displayed in Figs. 3a-3f for the case of $h_T = 100{,}000$ ft, $X_T = 80$ n.mi., $Y_T = 40$ n.mi., and standoff range $(R \times \beta)$ of 10 n.mi.

Figure 3a shows the ground track results. It appears that the vehicle completes the majority of the turn at the beginning of the flight. This stems from the fact that dynamic pressure and, as a result, the available lateral acceleration are the highest at the start. Note the alignment of the ground track with the target point at the 10 n.mi. standoff range. It is interesting that the *guidance/simulation* track is slightly "understeering" with respect to the others. This indicates that the approximate density used in the guidance computations is greater than the true from the standard atmosphere. The heading angle and side force coefficient plots (Figs. 3b and 3c) substantiate this behavior. χ increases rapidly at first and C_S is greatest at the initial time. The understeer in the simulation ground track results in a higher value for χ_f. In conjunction with this is the abrupt change in the final values of the approximate, optimal values of C_S in simulation, which is necessary to meet the end constraints.

The velocity results in Fig. 3d show a rapid bleed-off during the high-turn portion. To minimize the overall trajectory drag, it is necessary to sacrifice velocity at the beginning to take advantage of the peak dynamic pressure. The VFO2AD optimum final velocity appears to match that of the guidance simulation.

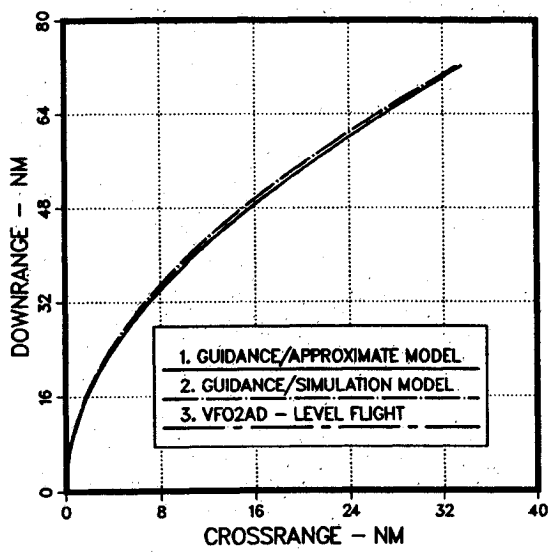

Fig. 3a Ground tracks.

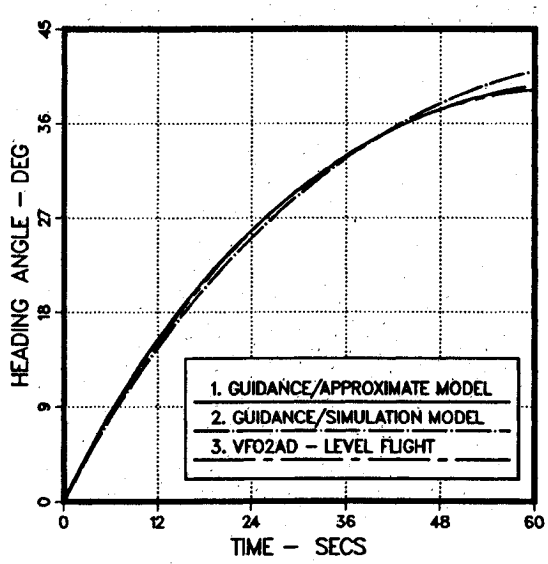

Fig. 3b Heading vs time.

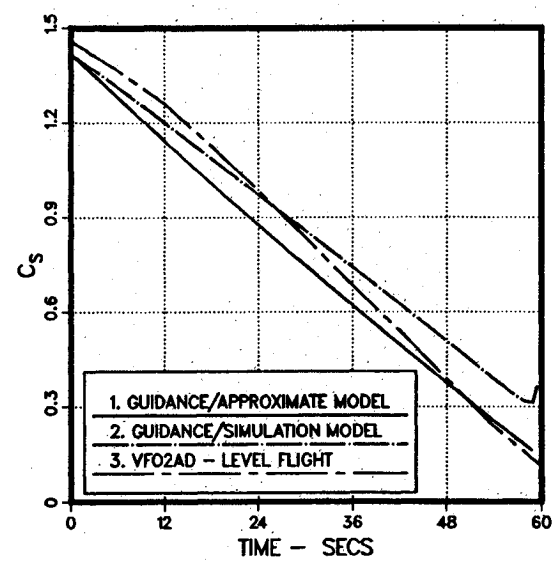

Fig. 3c Side force coefficient vs time.

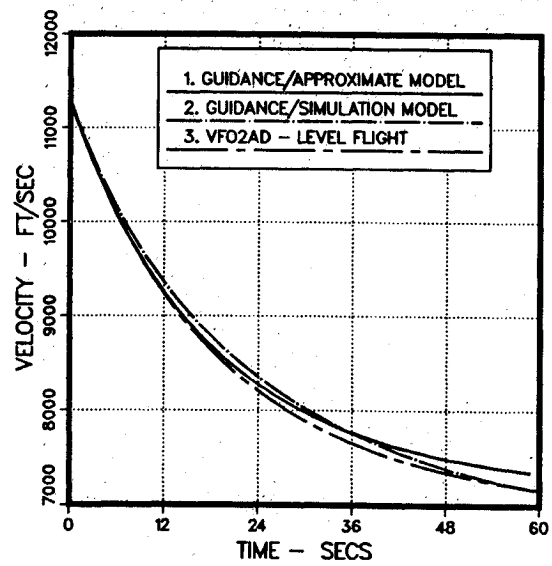

Fig. 3d Velocity vs time.

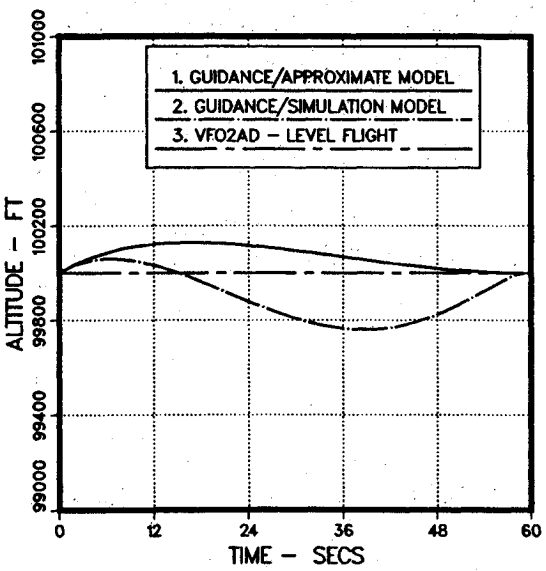

Fig. 3e Altitude vs time.

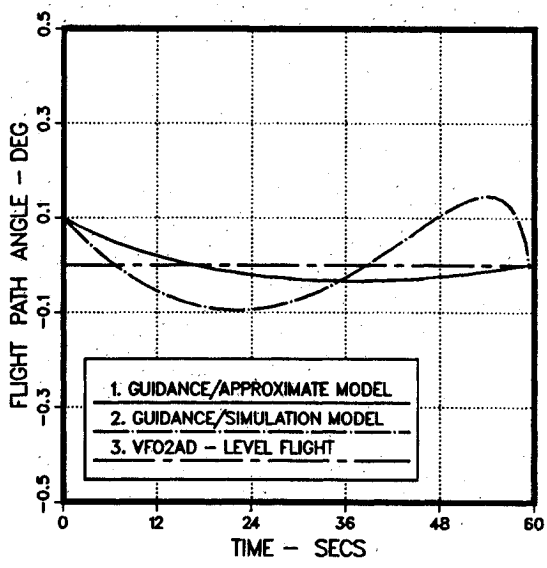

Fig. 3f Flight path angle vs time.

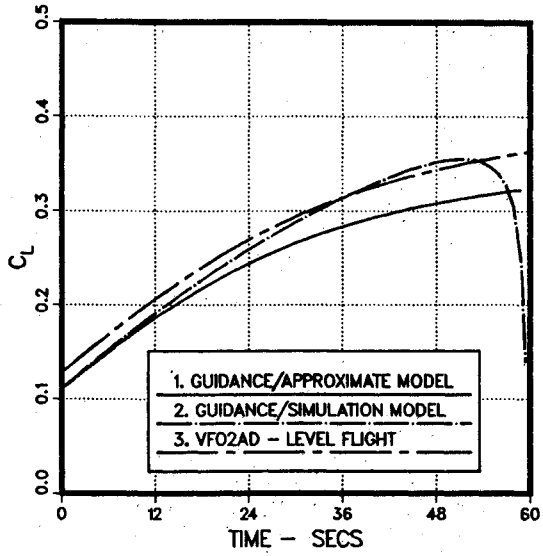

Fig. 3g Lift force coefficient vs time.

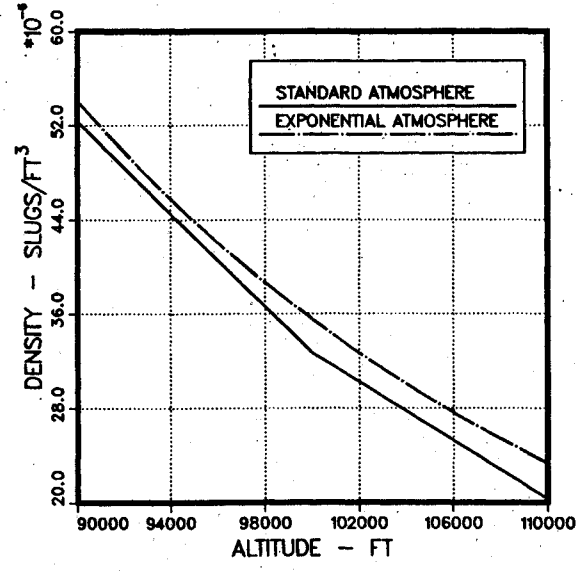

Fig. 4 Atmosphere comparison.

The altitude variation is shown in Fig. 3e. Although computations 1 and 2 start at $\gamma_0 = 0.1$ deg, the altitude excursions cover a band of less than 300 ft. Note that the incomplete knowledge of the atmosphere used by the guidance computations in simulation causes more maneuvering to meet the end conditions. The flight path angle variation in Fig. 3f remains small for the sample data applications, validating our initial assumption—although, as in the altitude comparison, the variation is more extensive in the simulation case. The end condition, $\gamma_f = 0$, is met in all cases. Lift coefficient results (Fig. 3g) show the real-time, optimal guidance corrections necessary to compensate for initial, nonzero flight path angles and atmospheric differences. Figure 4 has been included to compare the atmospheric densities for the example altitude region.

In general, as the standoff range to the target is increased, the terminal velocity decreases. Conversely, the limit case, $R = 0$, produces the absolute maximum at a given altitude. The solution for this case can be obtained directly with a reduced computational effort.

Conclusions

A guidance method has been presented to generate nearly constant-altitude, maximum terminal velocity trajectories to a fixed final position. Trajectories are characterized by high initial turn rates to take advantage of maximum dynamic pressure. Small deviations from constant-altitude flight appear correctable with negligible effect on performance. The approximate optimal guidance, in which the controls are repetitively computed based on updates at each sample point, compares well with a parameter optimization control solution. Guidance policies in simulation are able to compensate for atmospheric differences to meet end constraints.

References

[1]Eisler, G.R. and Hull, D.G., "Optimal, Descending Hypersonic Turn-to-Heading," *Journal of Guidance, Control, and Dynamics*, Vol. 10, May–June 1987, pp. 255–261.

[2]Miele, A., *Flight Mechanics, Vol. 1: Theory of Flight Paths*, Addison-Wesley, Reading, MA, 1962.

[3]Vinh, N.X., "Integrals of the Motion for Optimal Trajectories in Atmospheric Flight," *AIAA Journal*, Vol. 11, May 1973, pp. 700–703.

[4]Byrd, P.F. and Friedman, M.D., *Handbook of Elliptic Integrals for Engineers and Scientists*, 2nd ed., Springer-Verlag, Berlin, 1971.

[5]Speyer, J.L. and Hull, D.G., "Guidance and Control Synthesis for Hypersonic Gliders," Guidance and Control Group, Dept. of Aerospace Engineering, University of Texas, Austin, Dec. 1984.

[6]Powell, M.J.D., "A Fast Algorithm for Nonlinearly Constrained Optimization Calculations," *Proceedings of the Biennial Conference on Numerical Analysis*, Springer-Verlag, Berlin, 1978, pp. 144–157.

[7]Hull, D.G. and Speyer, J.L., "Optimal Reentry and Plane Change Trajectories," *Journal of the Astronautical Sciences*, Vol. XXX, No. 2, April–June 1982, pp. 117–130,